Journal of Hazardous Materials 181 (2010) 57–64

Contents lists available at ScienceDirect

Journal of Hazardous Materials

journal homepage: www.elsevier.com/locate/jhazmat

Decolorization of methylene blue by δ-MnO_2-coated montmorillonite complexes: Emphasizing redox reactivity of Mn-oxide coatings

Mao-Xu Zhu[a,*], Zheng Wang[a], Shao-Hui Xu[b], Tie Li[a]

[a] Key Laboratory of Marine Chemistry Theory and Technology, Ministry of Education, College of Chemistry and Chemical Engineering, Ocean University of China, No. 238, Songling Rd., Shandong Province, Qingdao 266100, China
[b] Department of Environmental Science and Engineering, Qingdao University, Qingdao 266071, China

ARTICLE INFO

Article history:
Received 20 January 2010
Received in revised form 30 March 2010
Accepted 19 April 2010
Available online 24 April 2010

Keywords:
δ-MnO_2 coatings
Montmorillonite
Methylene blue
Oxidative decolorization
Humic acid

ABSTRACT

δ-MnO_2 coatings on clay substrates tend to be poorer in crystallinity as compared with their discrete counterparts, which may be of environmental significance for adsorption and oxidation of contaminants. Discrete δ-MnO_2 particles and three δ-MnO_2-coated montmorillonite complexes with varying MnO_2 loadings (4.8–34.9%) were synthesized, and oxidative decolorization of methylene blue (MB) by the synthetic materials was investigated in batch systems. Results showed that oxidative decolorization of MB increased with increasing loading of Mn-oxide coatings, whereas oxidation capacity of the coatings, on the basis of unit mass of MnO_2, tended to decrease. Initial reaction rate of MB oxidation by both δ-MnO_2 coatings and their discrete counterpart increased linearly with increasing Mn-oxide loadings, but the rate of the former was higher than that of the latter. An increase in humic acid concentration displayed a progressively enhanced promotive effect on MB decolorization, whereas the promotive effect was greatly suppressed at lower pH.

1. Introduction

Manganese (Mn) oxides are ubiquitous in natural environments and exhibit versatility in regulating mobility and environmental fate of contaminants through adsorption, abiotic oxidation, catalytic transformation, or photochemical processes [1–4]. As far as abiotic oxidation is concerned, Mn oxides are among the strongest natural oxidants in soils and sediments with reducing potentials between 1.27 and 1.50 V. They are capable of oxidizing many inorganic contaminants [5–7], and a wide spectrum of natural and xenobiotic organic compounds such as catechol [1,8], quinines [9], substituted phenols [10], aromatic amines [11,12], phosphonates [13], antibacterial agents [14], antibiotics [15], brominated flame retardant [16], and steroid estrogens [17,18]. It has been reported that abiotic oxidation of a number of refractory organic contaminants by Mn oxides and subsequent polymerization are important pathways of their natural attenuation and immobilization in soils and sediments [8,12].

Natural Mn oxides may occur as discrete particles, small concretions/nodules, or coatings on surfaces of soils and sediments [2,19,20]. Manganese-oxide coatings on clay substrates, in particular on montmorillonite, are common in redox transition zones. A number of different mechanisms are involved in the formation of Mn-oxide coatings [2,21]. Natural and synthetic Mn-oxide coatings on clay minerals, silica, and alumina have been characterized using several techniques [22–24]. Those investigations have demonstrated that Mn-oxide coating changes substrate surface area, porosity, particle size, and surface electrochemical properties, which greatly influences sorption behavior of the substrates. Most importantly, interaction between Mn/Fe oxides with montmorillonite substrates can hinder even inhibit crystallization of Mn/Fe oxides [22,25], which may substantially enhance the density of reactive sites on Mn-oxide coating.

Adsorption behaviors of both discrete Mn oxides and Mn oxide-coated montmorillonite complexes for a number of inorganic ions have been extensively studied [26,27]. As oxidants, however, only discrete particles of Mn oxide have been tested to oxidize inorganic/organic contaminants [5,28,29]. Up to date, there is only limited information on redox reactivity of Mn-oxide coatings, though their redox importance in bulk soils and sediments has long been recognized [12,18].

It has been postulated that the formation of surface precursor complexes via adsorption on Mn oxides is the prerequisite to oxidation of organic compounds, and either surface complex formation or electron transfer is the rate-limiting step [9]. Some researchers found that oxidation kinetics of organic compounds during the initial stage followed a first- or pseudo-first-order rate with respect to the loss of target organic compounds, but deviated from the rate equation as the reaction proceeded [9,11,28]. However, a retarded first-order rate model was successfully employed to describe the

* Corresponding author. Tel.: +86 532 66782513; fax: +86 532 66782540.
E-mail address: zhumaoxu@ouc.edu.cn (M.-X. Zhu).

0304-3894/$ – see front matter © 2010 Elsevier B.V. All rights reserved.
doi:10.1016/j.jhazmat.2010.04.080

long-term oxidation of some organic compounds [15,16]. Most recently, a so-called MnOII kinetic model was developed to describe the entire time course of organic compound oxidation by Mn oxides [30].

Solution pH exerts critical impact on oxidation rate of organic compounds by Mn oxides by altering surface protonation/deprotonation and reducing potential of Mn oxides [28]. The effects of cosolutes on oxidation rate of inorganic/organic compounds by Mn oxides have been widely studied. Manganese(II) and to a lesser extent other metal cations such as Ca^{2+}, Zn^{2+}, Cu^{2+}, and Fe^{3+} at environmentally relevant concentrations display rate-inhibiting effect; however, humic acid was found to exhibit either promotive or inhibitive effect [9,17,31,32].

Given the potential decrease in crystallinity of Mn-oxide coatings on montmorillonite substrate, the objectives of this study were to evaluate oxidative decolorization of methylene blue (MB), a model organic pollutant, by Mn-oxide coatings through comparison with discrete δ-MnO_2, with an emphasis on redox reactivity of the coatings. The results are expected to add to our understanding on potential roles of natural Mn-oxide coatings in degradation of some anthropogenic organic contaminants in natural environments.

2. Materials and methods

2.1. Materials

Methylene blue (purity >98%) was purchased from Tianjin Guangcheng Chemical Reagent Co. Ltd., China, and used without further purification. All other employed chemicals are of analytical reagent grade. The chemical structure of MB was given previously [29].

Sodium-saturated montmorillonite (Na-Mt) used for the preparation of δ-MnO_2-coated montmorillonite (Mn-Mt) complexes was obtained from bentonite [33]. Humic acid (HA) used to evaluate its effect on oxidation of MB by Mn-oxide coatings was extracted from forest surface soil of the Qingdao Mountain according to Stevenson [34]. Organic carbon of the extracted HA was determined using a total carbon analyzer (Shimadzu Corp., Japan).

2.2. Preparation and characterization of δ-MnO_2 and Mn-Mt complexes

Discrete δ-MnO_2 and Mn-Mt complexes were prepared through a redox process [35]. $MnSO_4$ solution for the preparation of discrete δ-MnO_2, or well mixed suspensions containing constant amount of $MnSO_4$ but varying amounts of the Na-Mt (20.0, 3.33, and 2.00 g L^{-1}) for the preparation of Mn-Mt complexes, were added dropwise to mixtures of $KMnO_4$ (4.6×10^{-3} M) and NaOH (6.9×10^{-3} M) with the same volume as the $MnSO_4$ solution under motor-stirring and nitrogen purging. The precipitated Mn-oxide particles and Mn oxide-coated montmorillonite slurries were allowed to settle and age for 3 h. After aging, the resulting discrete δ-MnO_2 and Mn-Mt complexes were centrifuged and rinsed with deionized water and then re-dispersed in dilute KNO_3 solution (1.5×10^{-3} M) for 16 h. Finally, the discrete δ-MnO_2 and Mn-Mt complexes were centrifuged, rinsed, freeze-dried, and ground gently to pass a 100-mesh sieve for use. For brevity, the three Mn-Mt complexes with increasing Mn loadings are denoted hereafter as Mn-Mt-1, Mn-Mt-2 and Mn-Mt-3, respectively, and the discrete δ-MnO_2 denoted simply as DMO (Table 1).

The Na-Mt, DMO, and Mn-Mt complexes were subjected to X-ray diffraction (XRD) analysis on a Rigaku D/max-rB diffractometer (Rigaku Corp., Japan) (Cu Kα, 40 kV, 100 mA, 7° min^{-1}) and scanning electron microscopy (SEM) imaging (JEOL JSM-840). The amounts of Mn oxide loaded on the montmorillonites were evaluated by extraction using hydroxylamine hydrochloride–hydrochloric acid ($NH_2OH{\cdot}HCl$) [36]. The separated Mn filtrates through a 0.22-μm filter were immediately acidified with three droplets of 1:1 HNO_3 to around pH 1.0 and then stored at 4 °C until Mn measurement using flame atomic absorption spectroscopy (AAS) (Thermo Electron Co., USA). Zero point of charge (pH_{zpc}) of the DMO and Mn-Mt complexes was determined using a simplified method [37], and specific surface area and pore size distribution were determined by the BET method. Particle size distribution of the DMO and Mn-Mt was obtained using a laser-based particle size analysis (Laser 2000, UK) (Table 1).

2.3. Oxidative decolorization of MB

Oxidative decolorization of MB by the DMO and Mn-Mt complexes was carried out in batch reactors under conditions pertaining to natural soil environments: pHs from 4.0 to 5.5, HA contents from 12 and 30 mg organic carbon L^{-1}, and Mn-oxide loadings from 4.8% to 34.9%. It should be pointed out that higher contents of Mn oxides were used as compared with Mn contents in common soils and sediments (0.0061–25%) for the purpose of experimental convenience. Solution pHs were buffered using HAc–NaAc solutions with constant ΣAc^- concentration (0.05 M). It was found that acetate had only negligible effect on oxidation of many organic compounds [28,31]. Thus any potential effects of acetate on the systems were not taken into account in later discussion.

Fifty-milligram DMO or Mn-Mts were added to 100-mL conical flasks containing 25 mL MB of 80 mg L^{-1}. The suspensions were then gently shaken in a water bath at (27 ± 0.5) °C to pre-determined time intervals (10 min to 12.5 h). At each pre-determined time interval, the reactions were quenched using two methods (methods I and II) to yield oxidative loss of MB. In previous studies using MnO_2 as an oxidant, effort was made in some cases [15,32] and not in others [31,38] to separate oxidative fraction from adsorptive loss of organic compounds, and in the latter cases the total loss was simply used in kinetic modeling of oxidative reaction. In the present study, however, the separation of oxidative loss of MB from the total removal is critically important, because large surface area and low pH_{zpc} (2.81) of montmorillonite rendered MB cation sorption substantial, especially after reductive dissolution of Mn-oxide coatings.

Direct filtration separation (method I): aliquots of 15-mL suspensions were sampled using a syringe and immediately filtrated through a 0.22-μm syringe-end filter to separate the solid particles and thus stop further reaction in the filtrates. Methylene blue was immediately measured using a Hewlett-Packard 8453 UV–vis spectrophotometer at λ_{max} = 665 nm. Percent removal of MB, η, is defined as:

$$\eta(\%) = \left(1 - \frac{C_t}{C_0}\right) \times 100 \quad (1)$$

where C_0 is initial concentration of MB and C_t concentration at time t. In some selected systems, dissolved Mn(II) was measured to evaluate reductive dissolution of Mn oxides. Total percent removal of MB, η_T, using this quenching method was attributed to the sum of adsorptive removal and oxidative degradation.

Filtration separation after reductive dissolution (method II): excess amount of $NH_2OH{\cdot}HCl$ was added to the reaction systems to quickly dissolve all remaining DMO and Mn-oxide coatings. After complete dissolution, the suspensions in the Mn-Mt systems were filtrated (0.22 μm) and MB in the filtrates were immediately measured. Separate experiments confirmed that MB was stable in the presence of $NH_2OH{\cdot}HCl$ (with or without Mn^{2+}). In the DMO system,

Table 1
Basic properties of Na-Mt, DMO, and Mn-Mt complexes.

Sample	Na-Mt	Mn-Mt-1	Mn-Mt-2	Mn-Mt-3	DMO
pH_{zpc}	2.81	2.58	2.47	2.31	2.15
Predicted mass fraction of MnO_2 (%)	–	4.76	23.1	33.3	–
Extracted mass fraction of MnO_2 (%)	–	4.80	25.5	34.9	–
Specific surface area ($m^2\ g^{-1}$)	27.70	31.25	91.30	116.3	234.3
Pore diameter median (nm)	7.8	6.9	6.3	5.9	2.3
Particle size median (μm)	3.5	3.8	3.6	2.4	0.5

MB could be directly measured without filtration after dissolution of the Mn oxide.

After complete dissolution of Mn oxide, previously adsorbed MB on Mn oxides was released into solution. Thus the percent removal of MB in the DMO system, $\eta_{2(DMO)}$, was attributable to oxidative loss, $\eta_{ox(DMO)}$. In the Mn-Mt systems, however, the percent removal, $\eta_{2(Mn\text{-}Mt)}$, was attributable to the sum of oxidative degradation by the Mn-oxide coatings plus surface adsorption on the montmorillonite substrate. So a correction for MB adsorption on montmorillonite in all the Mn-Mt systems is needed in order to determine oxidative decolorization of MB, $\eta_{ox(Mn\text{-}Mt)}$.

For correction for MB adsorption on montmorillonite in the Mn-Mt systems containing varying masses of montmorillonite, MB adsorption on uncoated Na-Mt, $\eta_{Na\text{-}Mt}$, in the presence of Mn(II) ions was determined independently using uncoated Na-Mts whose masses were corresponding to those present in the Mn-Mt-1, Mn-Mt-2, and Mn-Mt-3, respectively. The presence of Mn(II) ions was important in the system because substantial amounts of Mn(II) ions would adsorb on montmorillonite once released from the Mn-Mt complexes [32], which would compete surface sites with MB. The concentration of Mn(II) used in each system was based on corresponding loadings of Mn oxide in the Mn-Mts. We assume MB oxidation by uncoated Na-Mt negligible in time scale of the experiments, though it has been reported that iron-bearing montmorillonite can oxidize phenols and aromatic amines, for instance, in a long duration [39]. The oxidation of Mn(II) ions by O_2 in the uncoated Na-Mt system during the experiments was expected trivial because of slow kinetics in acidic solution. The correction of $\eta_{ox(Mn\text{-}Mt)}$ for MB adsorption on montmorillonite in the Mn-Mt systems is made by:

$$\eta_{ox(Mn\text{-}Mt)} = \eta_{2(Mn\text{-}Mt)} - \eta_{Na\text{-}Mt} \quad (2)$$

It should be pointed out that the quantities of adsorbed MB on the uncoated Na-Mt are expected larger than on the montmorillonite present in the Mn-Mts because in the former system not all cosolutes present in the latter system were taken into account even though Mn(II) was included. For example, intermediate products of MB degradation were not included in the uncoated Na-Mt system. In the Mn-Mt systems, however, the intermediate products would compete with MB for adsorption sites and reduce MB adsorption. Thus the above correction would underestimate the oxidative decolorization to some extent. But this imperfection would not undermine the validity of the study because oxidative decolorization obtained under the circumstance of underestimation still played an important role in MB removal.

To evaluate the degree of MB mineralization, dissolved organic carbon (DOC) in two selected experimental runs (DMO and Mn-Mt-2) was determined using the same method for HA measurement. Similar to decolorization, DOC removal in solutions was also from contributions of both adsorption (non-degradation) and oxidation. Oxidative DOC removal (i.e., mineralization) was corrected for adsorption on the Na-Mt using the same method as that in the correction of the oxidative decolorization.

All the experiments were run in duplicate and data presented were averages of duplicate analysis.

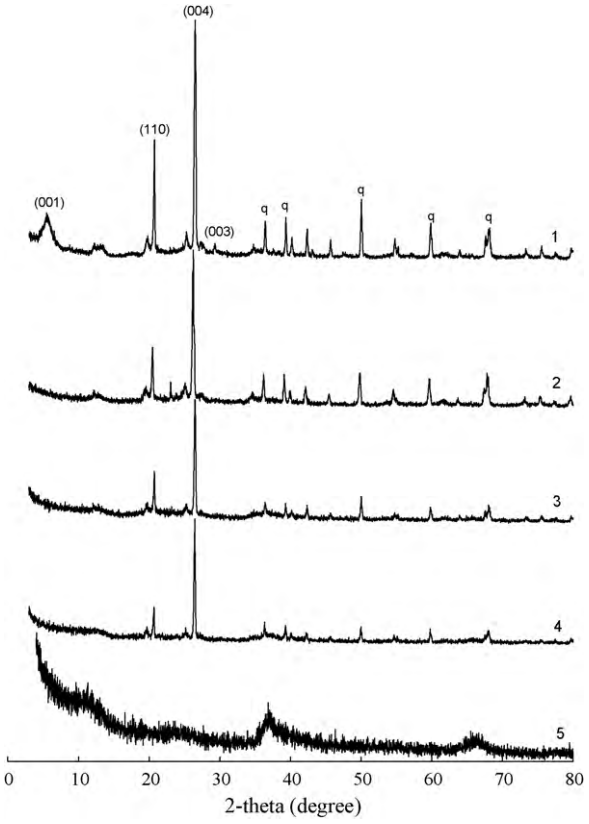

Fig. 1. X-ray diffraction patterns of Na-montmorillonite (Na-Mt), discrete δ-MnO_2 (DMO), and δ-MnO_2-coated montmorillonite (Mn-Mt) complexes. (1) Na-Mt, (2) Mn-Mt-1, (3) Mn-Mt-2, (4) Mn-Mt-3, and (5) DMO.

3. Results and discussion

3.1. Characterization of DMO and Mn-Mt complexes

As shown in Table 1, the loadings of Mn oxide on the Na-Mt were slightly higher than the theoretical values due probably to loss of montmorillonite colloids. The DMO has narrower range (from 0.1 μm to 40 μm) and smaller median value of particle sizes than the Na-Mt and Mn-Mt complexes (0.1–150 μm) (Table 1). As shown in Fig. 1, the DMO was poorly crystalline with a broad and weak XRD peak. With an increase in Mn loadings, all diffraction peaks of montmorillonite and quartz of the Mn-Mt complexes became progressively weaker even obscured. The (0 0 1) diffraction peak of montmorillonite almost completely disappeared after coated with even low Mn loading, which is similar to the observation of Boonfueng et al. [22]. The specific surface area of the DMO is generally within the values of δ-MnO_2 reported in literature. Specific surface areas of the Mn-Mt complexes ranged between those of the uncoated Na-Mt and the DMO, and substantially enhanced with an increase in Mn loadings as compared with the uncoated Na-Mt. The results may indicate that Mn loadings did not reach site saturation on interlayer and outer surfaces of the Na-Mt. A site

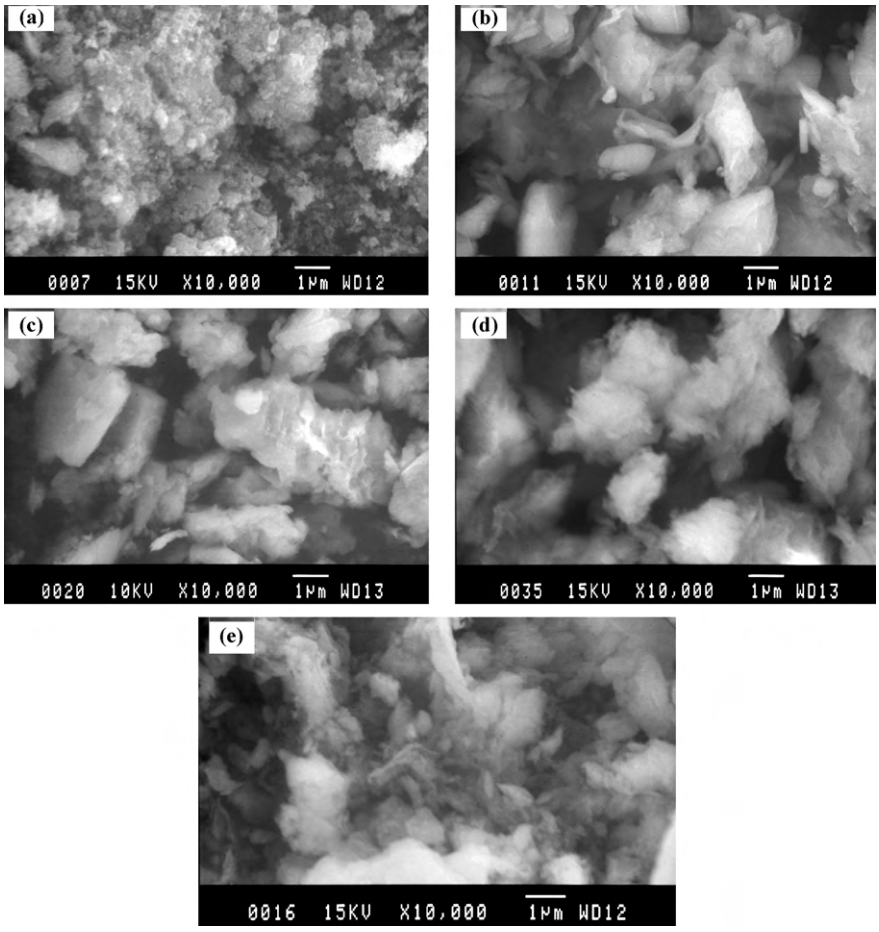

Fig. 2. SEM images of (a) DMO, (b) Na-Mt, (c) Mn-Mt-1, (d) Mn-Mt-2, and (e) Mn-Mt-3.

saturation effect was observed on montmorillonite with high Mn loadings [22], where surface properties of the complexes were predominantly determined by Mn-oxide end-member. The pH_{zpc} of the DMO is 2.15, slightly lower than the value (2.4) reported by Murray [35]. Similar to the specific surface area, the pHs_{zpc} of the Mn-Mt complexes are between those of the uncoated Na-Mt and the DMO, and increase with increasing Mn loadings. As given in Fig. 2, the DMO shows fine-sized, aggregated morphology. The Na-Mt is of massive aggregates in morphology, flakes were also observed. The morphology of the Mn-Mt-1 is similar to that of the Na-Mt, but the surfaces of the former are somewhat coarser. The Mn-Mt-2 is not quite different from the Na-Mt and the Mn-Mt-1 in particle sizes, but shows acicular texture on the surfaces. The acicular texture was also observed on the Mn-Mt-3, but the particle sizes were smaller in comparison with the Mn-Mt-1 and Mn-Mt-2.

3.2. Effect of Mn-oxide loading on oxidative decolorization of MB

The total (η_T) and oxidative (η_{ox}) decolorization of MB at pH 4.0 followed similar time course (Fig. 3): a quick increase in the initial stage followed by a slow process in the later stage. At any given time, the η_T followed the order (Fig. 3a): DMO > Mn-Mt-3 > Mn-Mt-2 > Mn-Mt-1 > Na-Mt. The η_{ox} also increased with increasing Mn loadings (Fig. 3b). The η_{ox} in the DMO system approached 100% within 5 h due to high Mn-oxide mass; in the Mn-Mt-2 and Mn-Mt-3 systems the η_{ox} increased gradually for quite a long time after the initial quick increase (>10 h). At low Mn loading (Mn-Mt-1), however, the η_{ox} was less than 20% and remained almost constant after the short initial stage. In the DMO system, simultaneous approach to 100% of both the η_T and η_{ox} over 5 h indicates complete decolorization mainly via oxidation. In the three Mn-Mt systems the η_{ox} was lower than the corresponding η_T, implying that a fraction of the η_T was from the contribution of adsorption on surfaces.

The increase in the η_{ox} with increasing Mn loadings is consistent with previous postulation that oxidative degradation of organic compounds is via a surface mechanism [9,28]. It follows that surface reactivity and density of available adsorption sites are two critical factors controlling oxidative decolorization of MB. The increase in Mn loadings on Na-Mt can enhance reactive sites available for adsorption and thereby for MB oxidation. The gradual increase in the η_{ox} in the later stage in the Mn-Mt-2 and Mn-Mt-3 systems could be attributed to hindrance of MB diffusion through micropores to react with interlayer Mn-oxide coatings. This retardation effect was not observed in the Mn-Mt-1 due probably to low Mn loading. It can be inferred that outer Mn-oxide coatings on the three Mn-Mts became depleted over relatively short duration of reaction.

The comparison of oxidative decolorization and oxidative DOC removal is shown in Fig. 4. In the initial stage, the oxidative decolorization was much higher than the oxidative DOC removal, but the latter approached gradually the former in the later stage, suggesting that the decolorization (i.e., breakdown of chromophoric moieties) was the preferential process of the degradation, followed by slow mineralization of intermediate products. For the purpose of characterizing redox reactivity of Mn-oxide coatings at the initial stage, it is therefore more appropriate to use the rate of oxidative decolorization rather than the rate of oxidative DOC removal. In the following parts, our discussion is mainly based on the data of oxidative decolorization.

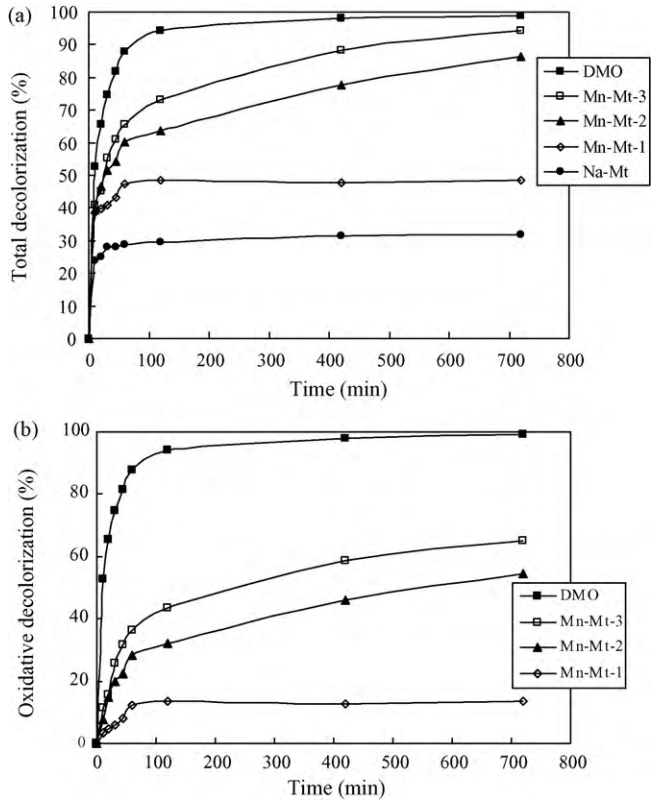

Fig. 3. Effect of MnO_2 loading on total (a) and oxidative (b) decolorization of methylene blue (MB).

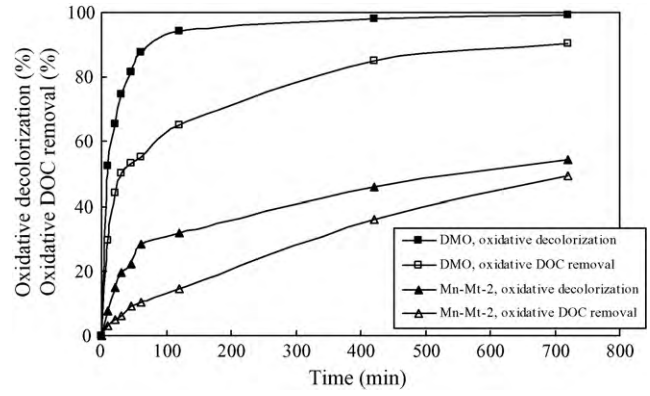

Fig. 4. Comparison of oxidative decolorization and oxidative DOC removal in systems of DMO and Mn-Mt-2.

To compare the oxidation capability of Mn-oxide coatings among the Mn-Mts and DMO, MB oxidation capacities (% MB g^{-1} MnO_2) in terms of unit mass of Mn oxide were calculated and compared in Fig. 5. Interestingly, the Mn-Mt-1 exhibited the highest oxidation capability, followed by the Mn-Mt-2 and Mn-Mt-3, and the DMO was the lowest in the capability. This trend could only be explained by different crystallinity of the Mn oxides, and thereby their different adsorption affinity and redox reactivity. It has been reported that the presence of montmorillonite substrate results in more poorly crystalline birnessite coatings and potentially inhibits crystallization of pyrolusite which otherwise well crystallizes in the absence of the substrate [22]. The decrease in crystallinity of Mn oxides will result in an enhancement in both specific surface area and redox reactivity. Unfortunately, the specific surface area of the Mn-oxide coatings on the montmorillonite could not be independently determined to confirm the postulation. The highest oxidation capacity of the Mn-oxide coatings on the Mn-Mt-1 implies that the inhibitive effect on crystallization of the Mn-oxide coatings tends to be larger at lower density of Mn oxides on the surfaces. However, a simple conclusion like this could not be reached because the oxidation capacities between the Mn-Mt-2 and Mn-Mt-3 were similar and were not markedly larger than in the DMO system despite obvious differences in Mn-oxide contents among them (Fig. 5).

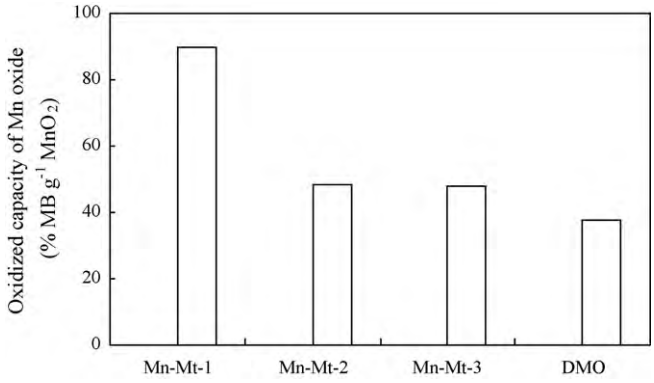

Fig. 5. Oxidizing capacities (on the basis of unit mass of MnO_2) of discrete δ-MnO_2 (DMO) and δ-MnO_2 coatings in oxidative decolorization of methylene blue (MB).

Table 2
Initial rate constants in DMO, Mn-Mt systems calculated on the basis of pseudo-first-order rate equations.

Samples	Solid phase conc. ($g\,L^{-1}$)	MnO_2 conc. ($g\,L^{-1}$)	Initial rate constant k (min^{-1})	R^2
Mn-Mt-1	0.200	0.011	0.0019	0.9563
DMO	0.011	0.011	0.0015	0.9808
Mn-Mt-2	0.200	0.051	0.0049	0.9603
DMO	0.051	0.051	0.0042	0.9949
Mn-Mt-3	0.200	0.070	0.0068	0.9674
DMO	0.070	0.070	0.0054	0.9626

R: correlation coefficient.

3.3. Initial kinetic rate of oxidative decolorization of MB

In this study, kinetic experiments were undertaken to compare the initial rate of MB oxidation in the Mn-Mt and DMO systems at three Mn levels (Table 2). Preliminary results demonstrated that MB oxidation by the DMO well followed a pseudo-first-order kinetics within 60 min. Thus this type of rate equation was used to yield the initial kinetic rate with respect to oxidative loss of MB in the systems studied. The initial kinetic rates were determined from the slopes in the plot of logarithmetic concentration of MB versus time within 60 min. The initial rate constants in the Mn-Mt systems were larger than in the corresponding DMO systems (Table 2), which further confirmed the earlier conclusion that redox reactivity of the Mn-oxide coatings was higher than that of their discrete counterpart under otherwise identical conditions. For both the Mn-oxide coatings and DMO, the initial rate constants increased linearly as a function of Mn-oxide quantity (Fig. 6), suggesting that the kinetic rate was directly proportional to the total surface areas of the Mn oxides, and thereby to the concentration of surface complexes, as suggested by Xyla et al. [40].

3.4. Effect of pH on oxidative and adsorptive decolorization of MB

A selected sample (Mn-Mt-2) was used to evaluate the effect of pH on η_T and η_{ox} of MB in the Mn-Mt systems, where the initial concentration of MB was 80 mg L^{-1} and Mn-Mt-2 dosage 50 mg.

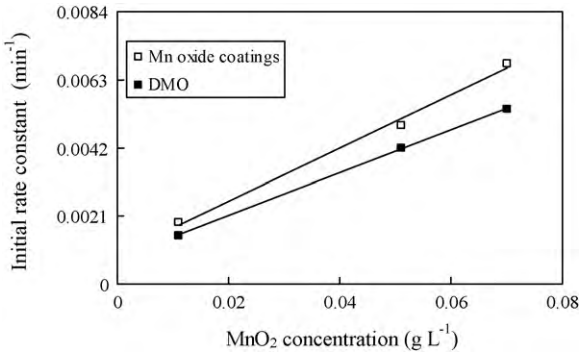

Fig. 6. Initial rate constants of methylene blue (MB) oxidation as a function of Mn-oxide contents.

After the initial reaction stage, the η_T and η_{ox} decreased with an increase in pH (Fig. 7).

Besides exerting an influence on surface charge density of Mn oxides and on species distribution of ionizable adsorbates, pH also influences reducing potential of Mn oxides in reaction (3) according to the Nernst Equation:

$$\delta\text{-}MnO_2(s) + 4H^+ \rightleftharpoons Mn^{2+}(aq) + 2H_2O \quad \varphi^\circ(MnO_2/Mn^{2+}) = 1.23\,V \tag{3}$$

The surfaces of all the Mn-Mts are negatively charged due to lower H_{zpc} (2.31–2.58) (Table 1) than suspension pH (4.0–5.5) of this study, and the negative charge density increased with increasing pH, which was conducive to adsorption of MB cations and thereby to the formation of surface complexes. However, the η_T and η_{ox} decreased with increasing pH (Fig. 7a and b), suggesting that the increase in density of surface complexes was not the predominant factor controlling oxidative decolorization of MB. As a matter of fact, a decrease in pH would cause an increase in reducing potential of Mn oxides according to the Nernst Equation. Thus pH exerted a double-edged effect on MB oxidation by controlling surface complex formation and Mn-oxide reducing potential. The larger η_{ox} at lower pH than at higher pH suggested that pH effect on reducing potential outcompeted its effect on surface complexation. The increase in Mn(II) concentration as reaction proceeded was an indicative of oxidative decolorization of MB (Fig. 7c) because in the absence of MB, dissolved Mn(II) was under detection limit at the two pHs. It should be pointed out, however, that the higher Mn(II) concentration at pH 4.0 than at pH 5.5 was not solely caused by elevated reductive dissolution at lower pH, but was superimposed on by suppressed adsorption of Mn(II) due to enhanced protonation.

Adsorption of MB cations on montmorillonite was expected to decrease with decreasing pH due to increased protonation and competitive effect of Mn(II). However, the consistent increase in η_T and η_{ox} with decreasing pH implied that oxidative loss of MB was predominantly responsible for the total loss of MB.

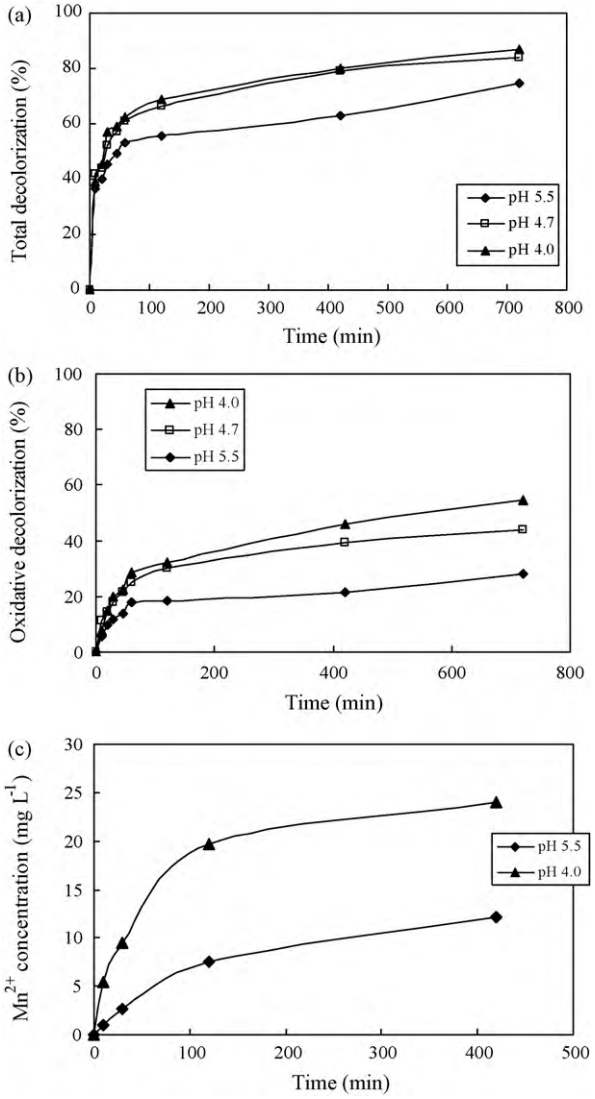

Fig. 7. Effect of pH on total (a) and oxidative (b) decolorization of methylene blue (MB) by Mn-Mt-2, and dissolved Mn(II) concentration as a function of time at pH 4.0 and 5.5 (c).

3.5. *Effect of HA cosolute on total decolorization of MB by Mn-Mt complexes*

The effects of HA on η_T of MB in a selected Mn-Mt system (Mn-Mt-2) at two conditions: (i) fixed pH (4.0) but varying HA levels (12 and 30 mg organic carbon L^{-1}), and (ii) fixed HA level but varying pHs (4.0 and 5.5) were investigated, but η_{ox} could not be determined because $NH_2OH{\cdot}HCl$ is incapable of effectively eliminating Mn-oxide coatings in the presence of HA due probably to interaction between HA and $NH_2OH{\cdot}HCl$ or protection of Mn-oxide coatings by HA. Nevertheless, given the predominant contribution of the η_{ox} to the η_T as inferred earlier as well as similar pH dependency between them, the η_T could be lent as a proxy to illustrate the η_{ox} approximately. As shown in Fig. 8a, the η_T was enhanced in the presence of elevated HA concentration, suggesting a promotive effect. Notice that, in the Na-Mt system, the η_T was very low in the presence of HA as compared with that in the Mn-Mt-2 system. This was due to competitive adsorption between MB and HA as well as the absence of MB oxidation in the former system.

Humic acid has been found to exhibit either promotive or inhibitive effect on oxidation of organics by Mn oxides. A notable decrease was observed in degradation of a number of organic compounds in the presence of even low HA concentrations and attributed the inhibitive effect to direct competition for reactive sites as well as reductive dissolution of MnO_2 by HA. Reductive dissolution of MnO_2 by HA produces Mn(II) as a strong inhibitor [9,31,32]. Xu et al. [17], however, found that the presence of HA pronouncedly enhanced oxidative removal of estrogens and attributed the promotive effect to Mn(II)–HA complexation as well as refractory nature of the HA (i.e., incapable of reductively dissolving Mn oxides), thereby suppressing competitive adsorption of Mn(II) with the organic compounds.

It appears that Mn(II)–HA complexation in this study has outcompeted reductive dissolution of Mn oxide by HA. Given the fact that HA generally displays high affinity for metal cations including Mn(II), redox reactivity of HA may be the key factor determining

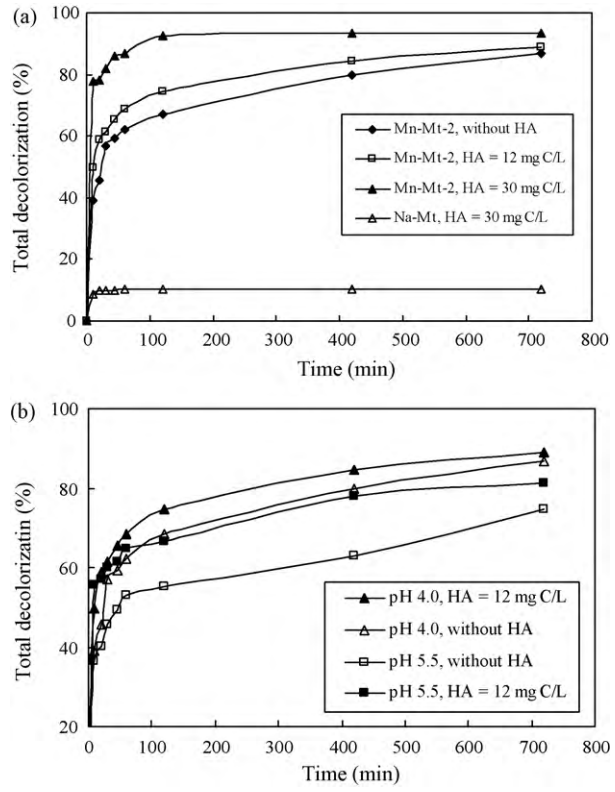

Fig. 8. (a) Effect of humic acid (HA) concentration at fixed pH (4.0) on total decolorization of methylene blue (MB) by Mn-Mt-2 and Na-Mt and (b) effect of HA on total decolorization of MB by Mn-Mt-2 at pH 4.0 and 5.5.

its promotive/inhibitive effects. Natural HA indeed displays a wide range of redox reactivity, depending on its genesis. Humic acid from some sources may be capable of reductively dissolving Mn oxide to different extents, however, HA from other sources may be much recalcitrant. As a matter of fact, Mn oxides play an important role in polymerization and formation of HA in some cases [41]. Therefore, HA may exhibit either inhibitive or promotive effect on oxidation of organic compounds, depending on its redox reactivity, and it is not surprising that contrary effects (promotive versus inhibitive) have been observed among authors.

The promotive effect at pH 5.5 was more obvious than at pH 4.0, at which only a slight enhancement was observed (Fig. 8b). This trend was likely a combined result of lower sorption of HA on surface sites [42] together with weak reductive dissolution of Mn oxides at higher pH, which was expected to render higher concentrations of HA in solution and thereby higher Mn(II)–HA complexation.

Combining this study and previous observations, we might conclude that several factors, including redox reactivity of HA, HA adsorption, Mn(II) adsorption versus Mn(II)–HA complexation, all influenced by pH, jointly determined the effect of HA on oxidative removal of target organic compounds by Mn oxides.

3.6. Geochemical implications of Mn-oxide coatings

To best of the authors' knowledge, this is the first to report that Mn-oxide coatings exhibit higher capability and faster initial kinetic rate for oxidation of MB as compared with their discrete counterpart. Such elevated redox reactivity is expected to hold for naturally occurring Mn-oxide coatings in abiotic oxidation of many other organic contaminants. Besides Mn oxides, iron oxides are also important electron acceptors and commonly occur as coatings on montmorillonite and sand substrates. Decreased crystallinity of iron-oxide coatings on clay substrates has been also reported [25,43]. Iron-oxide coatings may also exhibit elevated redox reactivity as compared with their discrete counterparts, which may also be of environmental significance.

In previous laboratory studies on oxidation of organic pollutants by Mn oxides, synthetic discrete particles of Mn oxides with varying crystallinities have been commonly employed. Those results may have underestimated to some extent the oxidation capability and initial kinetic rate of Mn oxides naturally occurring as coatings to oxidize organic compounds, which, if true, will compromise the validity of dynamic models established on the basis of kinetic data only from discrete Mn oxides for the prediction of environmental fate of organic pollutants in soils and sediments.

4. Conclusion

Mn-oxide coatings exhibit higher capability and faster initial kinetic rate for the oxidation of MB as compared with their discrete counterpart. The total oxidative decolorization of MB by Mn-oxide coatings increased with enhanced Mn loadings, whereas oxidation capacity on the basis of unit mass of MnO_2 tended to decrease with increased density of the coatings on the montmorillonite substrate. pH exerts an important effect on redox potential of Mn-oxide coatings and a decrease in pH from 5.5 to 4.0 can greatly enhance oxidative decolorization of MB. Initial kinetic rates of MB oxidation by δ-MnO_2 coatings and their discrete counterparts increase linearly with Mn-oxide loading, with the former higher than the latter. Humic acid cosolute display a progressively enhanced promotive effect on MB decolorization with increased HA concentrations, whereas the promotive effect is much suppressed at lower pH. For more accurate prediction of natural attenuation of organic pollutants in soils and sediments rich in Mn-oxide coatings, elevated oxidation capacity and initial kinetic rate of Mn-oxide coatings as compared with discrete δ-MnO_2 particles have to be taken into account.

Acknowledgments

This work was financially supported by the NSF of China (Grant No. 40771095), the Scientific Research Foundation for the Returned Overseas Chinese Scholars, the State Education Ministry, and the Subsidy Funds of Personnel Training of China National Fundamental Fund Project (J0730530).

References

[1] C.J. Matocha, D.L. Sparks, J.E. Amonette, R.K. Kukkadapu, Kinetics and mechanism of birnessite reduction by catechol, Soil Sci. Soc. Am. J. 65 (2001) 58–66.
[2] D. Dong, L.A. Derrym, L.W. Lion, Pb scavenging from a freshwater lake by Mn oxides in heterogeneous surface coating materials, Water Res. 37 (2003) 1662–1666.
[3] S.W.C. Chien, H.L. Chen, M.C. Wang, K. Seshaiah, Oxidative degradation and associated mineralization of catechol, hydroquinone and resorcinol catalyzed by birnessite, Chemosphere 74 (2009) 1125–1133.
[4] K.D. Kwon, K. Refson, G. Sposito, On the role of Mn(IV) vacancies in the photoreductive dissolution of hexagonal birnessite, Geochim. Cosmochem. Acta 73 (2009) 4142–4150.
[5] R. Dai, J. Liu, C. Yu, R. Sun, Y. Lan, J.-D. Mao, A comparative study of oxidation of Cr(III) in aqueous ions, complex ions and insoluble compounds by manganese-bearing mineral (birnessite), Chemosphere 76 (2009) 536–541.
[6] V.Q. Chiu, J.G. Hering, Arsenic adsorption and oxidation at manganite surfaces. 1. Method for simultaneous determination of adsorbed and dissolved arsenic species, Environ. Sci. Technol. 34 (2000) 2029–2034.
[7] M.J. Scott, J.J. Morgan, Reactions at oxide surfaces. 2. Oxidation of Se(IV) by synthetic birnessite, Environ. Sci. Technol. 30 (1996) 1990–1996.
[8] M.L. Colarieti, G. Toscano, M.R. Ardi, G. Greco Jr., Abiotic oxidation of catechol by soil metal oxides, J. Hazard. Mater. 134 (2006) 161–168.
[9] A.T. Stone, J.J. Morgan, Reduction and dissolution of manganese (III) and manganese (IV) oxides by organics: 1. Reaction with hydroquinone, Environ. Sci Technol. 18 (1984) 450–456.

[10] R.A. Petrie, P.R. Grossl, R.C. Sims, Oxidation of pentachlorophenol in manganese oxide suspensions under controlled *E*h and pH environments, Environ. Sci. Technol. 36 (2002) 3744–3748.
[11] S. Laha, R.G. Luthy, Oxidation of aniline and other primary aromatic amines by manganese dioxide, Environ. Sci. Technol. 24 (1990) 363–373.
[12] H. Li, L.S. Lee, D.G. Schulze, C. Guest, Role of soil manganese in the oxidation of aromatic amines, Environ. Sci. Technol. 37 (2003) 2686–2693.
[13] K.A. Barrett, M.B. McBride, Oxidative degradation of glyphosate and aminomethylphosphonate by manganese oxide, Environ. Sci. Technol. 39 (2005) 9223–9228.
[14] H. Zhang, C.-H. Huang, Oxidative transformation of fluoroquinolone antibacterial agents and structurally related amines by manganese oxide, Environ. Sci. Technol. 39 (2005) 4474–4483.
[15] K.F. Rubert, J.A. Pedersen, Kinetics of oxytetracycline reaction with a hydrous manganese oxide, Environ. Sci. Technol. 40 (2006) 7216–7221.
[16] K. Lin, W. Liu, J. Gan, Reaction of tetrabromobisphenol A (TBBPA) with manganese dioxide: kinetics, products, and pathways, Environ. Sci. Technol. 43 (2009) 4480–4486.
[17] L. Xu, C. Xu, M. Zhao, Y. Qiu, G.D. Sheng, Oxidative removal of aqueous steroid estrogens by manganese oxides, Water Res. 42 (2008) 5038–5044.
[18] G.D. Sheng, C. Xu, L. Xu, Y. Qiu, H. Zhou, Abiotic oxidation of 17β-estradiol by soil manganese oxides, Environ. Pollut. 157 (2009) 2710–2715.
[19] K.A. Hudson-Edwards, M.G. Macklin, C.D. Curtis, D.J. Vaughan, Processes of formation and distribution of Pb-, Zn-, Cd-, and Cu-bearing minerals in the Tyne Basin. Northeast England: implications for metal contaminated river systems, Environ. Sci. Technol. 30 (1996) 72–80.
[20] F. Liu, C. Colombo, J.Z. He, A. Violante, Trace elements in manganese-iron nodules from a Chinese Alfisol, Soil Sci. Soc. Am. J. 66 (2002) 661–671.
[21] Y. Tani, N. Miyata, K. Iwahori, M. Soma, S. Tokuda, H. Seyama, B.K.G. Theng, Biogeochemistry of manganese oxide coatings on pebble surfaces in the Kikukawa River System, Shizuoka, Japan, Appl. Geochem. 18 (2003) 1541–1554.
[22] T. Boonfueng, L. Axe, Y. Xu, Properties and structure of manganese oxide-coated clay, J. Colloid Interface Sci. 281 (2005) 80–92.
[23] R. Han, W. Zou, Z. Zhang, J. Shi, J. Yang, Removal of copper(II) and lead(II) from aqueous solution by manganese oxide coated sand I. Characterization and kinetic study, J. Hazard. Mater. 137 (2006) 384–395.
[24] S.M. Maliyekkal, A.K. Sharma, L. Philip, Manganese-oxide-coated alumina: a promising sorbent for defluoridation of water, Water Res. 40 (2006) 3497–3506.
[25] H. Green-Pedersen, N. Pind, Preparation, characterization, and sorption properties for Ni(II) of iron oxyhydroxide-montmorillonite, Colloids Surf. A 168 (2000) 133–145.
[26] T. Boonfueng, L. Axe, Y. Xu, T.A. Tyson, Nickel and lead sequestration in manganese oxide-coated montmorillonite, J. Colloid Interface Sci. 303 (2006) 87–98.
[27] A. Turner, S.M. Le Roux, G.E. Millward, Adsorption of cadmium to iron and manganese oxides during estuarine mixing, Mar. Chem. 108 (2008) 77–84.
[28] A.T. Stone, Reduction dissolution of manganese (III/IV) oxides by substituted phenols, Environ. Sci. Technol. 2 (1987) 1979–1988.
[29] M.-X. Zhu, Z. Wang, L.-Y. Zhou, Oxidative decolorization of methylene blue using pelagite, J. Hazard. Mater. 150 (2008) 37–45.
[30] H. Zhang, W.-R. Chen, C.-H. Huang, Kinetic modeling of oxidation of antibacterial agents by manganese oxide, Environ. Sci. Technol. 42 (2008) 5548–5554.
[31] J. Klausen, S.B. Haderlein, R.P. Schwarzenbach, Oxidation of substituted anilines by aqueous MnO_2: effect of co-solute on initial and quasi-steady-state kinetics, Environ. Sci. Technol. 31 (1997) 2642–2649.
[32] H. Zhang, C.-H. Huang, Oxidative transformation of triclosan and chlorophene by manganese oxides, Environ. Sci. Technol. 37 (2003) 2421–2430.
[33] M.-X. Zhu, M. Xie, X. Jiang, Interaction of fluoride with hydroxyaluminum-montmorillonite complexes and implications for fluoride-contaminated acidic soils, Appl. Geochem. 21 (2006) 675–683.
[34] F.J. Stevenson, Humus Chemistry, John Wiley & Sons, New York, 1982.
[35] J.W. Murray, Surface chemistry of hydrous manganese dioxide, J. Colloid Interface Sci. 46 (1974) 357–371.
[36] T.T. Chao, Selective dissolution of manganese oxides from soils and sediments with acidified hydroxylamine hydrochloride, Soil Sci. Soc. Am. J. 36 (1972) 764–768.
[37] Y. Wang, E.J. Reardon, Activation and regeneration of a soil sorbent for defluoridation of drinking water, Appl. Geochem. 16 (2001) 531–539.
[38] K.-H. Kang, D.-M. Lim, H. Shin, Oxidative-coupling reaction of TNT reduction products by manganese oxide, Water Res. 40 (2006) 903–910.
[39] C.C. Ainsworth, B.D. McVeety, S.C. Smith, J.M. Zachara, Transformation of 1-aminonapththalene at the surface of smectite clays, Clays Clay Miner. 39 (1991) 416–427.
[40] A.G. Xyla, B. Sulzberger, G.W. Luther III, J.G. Hering, P. van Cappellen, W. Stumm, Reduction dissolution of manganese(III, IV) (hydr)oxides by oxalate: the effect of pH and light, Langmuir 8 (1992) 95–103.
[41] A. Jokie, A.I. Frenkel, M.A. Vairavamurhy, P.M. Huang, Birnessite catalysis of the Maillard reaction: its significance in natural humification, Geophys. Res. Lett. 28 (2001) 3899–3902.
[42] W. Stumm, J.J. Morgan, Aquatic Chemistry, third ed., Wiley, New York, 1996.
[43] U. Schwertmann, The influence of aluminum on iron oxides: 5. Clay minerals as sources of aluminum, Soil Sci. 128 (1979) 195–200.